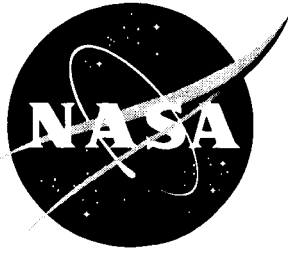


NASA/TM-2003-212645



Progress in the Phase 0 Model Development of a STAR Concept for Dynamics and Control Testing

Jessica A. Woods-Vedeler
Langley Research Center, Hampton, Virginia

Sasan C. Armand
SWALES Aerospace Corporation, Hampton, Virginia

The NASA STI Program Office . . . in Profile

Since its founding, NASA has been dedicated to the advancement of aeronautics and space science. The NASA Scientific and Technical Information (STI) Program Office plays a key part in helping NASA maintain this important role.

The NASA STI Program Office is operated by Langley Research Center, the lead center for NASA's scientific and technical information. The NASA STI Program Office provides access to the NASA STI Database, the largest collection of aeronautical and space science STI in the world. The Program Office is also NASA's institutional mechanism for disseminating the results of its research and development activities. These results are published by NASA in the NASA STI Report Series, which includes the following report types:

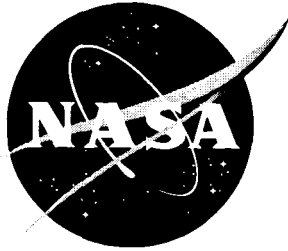
- **TECHNICAL PUBLICATION.** Reports of completed research or a major significant phase of research that present the results of NASA programs and include extensive data or theoretical analysis. Includes compilations of significant scientific and technical data and information deemed to be of continuing reference value. NASA counterpart of peer-reviewed formal professional papers, but having less stringent limitations on manuscript length and extent of graphic presentations.
- **TECHNICAL MEMORANDUM.** Scientific and technical findings that are preliminary or of specialized interest, e.g., quick release reports, working papers, and bibliographies that contain minimal annotation. Does not contain extensive analysis.
- **CONTRACTOR REPORT.** Scientific and technical findings by NASA-sponsored contractors and grantees.
- **CONFERENCE PUBLICATION.** Collected papers from scientific and technical conferences, symposia, seminars, or other meetings sponsored or co-sponsored by NASA.
- **SPECIAL PUBLICATION.** Scientific, technical, or historical information from NASA programs, projects, and missions, often concerned with subjects having substantial public interest.
- **TECHNICAL TRANSLATION.** English-language translations of foreign scientific and technical material pertinent to NASA's mission.

Specialized services that complement the STI Program Office's diverse offerings include creating custom thesauri, building customized databases, organizing and publishing research results ... even providing videos.

For more information about the NASA STI Program Office, see the following:

- Access the NASA STI Program Home Page at <http://www.sti.nasa.gov>
- E-mail your question via the Internet to help@sti.nasa.gov
- Fax your question to the NASA STI Help Desk at (301) 621-0134
- Phone the NASA STI Help Desk at (301) 621-0390
- Write to:
NASA STI Help Desk
NASA Center for AeroSpace Information
7121 Standard Drive
Hanover, MD 21076-1320

NASA/TM-2003-212645



Progress in the Phase 0 Model Development of a STAR Concept for Dynamics and Control Testing

Jessica A. Woods-Vedeler
Langley Research Center, Hampton, Virginia

Sasan C. Armand
SWALES Aerospace Corporation, Hampton, Virginia

National Aeronautics and
Space Administration

Langley Research Center
Hampton, Virginia 23681-2199

September 2003

Available from:

NASA Center for Aerospace Information (CASI)
7121 Standard Drive
Hanover, MD 21076-1320
(301) 621-0390

National Technical Information Service (NTIS)
5285 Port Royal Road
Springfield, VA 22161-2171
(703) 605-6000

PROGRESS IN THE PHASE 0 MODEL DEVELOPMENT OF A STAR CONCEPT FOR DYNAMICS AND CONTROL TESTING

Jessica A. Woods-Vedeler
NASA Langley Research Center
Sasan C. Armand
SWALES Aerospace Corporation

ABSTRACT

The paper describes progress in the development of a lightweight, deployable passive Synthetic Thinned Aperture Radiometer (STAR). It is envisioned the spacecraft concept presented will enable the realization of 10 km resolution global soil moisture and ocean salinity measurements at 1.41 GHz. The focus of this work was on definition of an approximately 1/3-scaled Phase 0 test article (5 meter aperture) for concept demonstration and dynamics and control testing. In particular, design requirements and parameters for a dynamically scaled test model were established based on related full scale mission concepts. A trade study was performed to identify a multi-parameter, hybrid scaling approach. As part of this, it was shown via analysis that if the mass of the lightweight structural components is small within the overall system, the dominant parameter for dynamic scaling of thin shelled structural members is bending stiffness, EI. Thus, the approach includes an EI Scaling Approach that allows freedom to design the cross section of scaled model components most conveniently for manufacturing. In addition, initial analysis of the Phase 0 test model was conducted to optimize the geometry of the panel for optimal load distribution. Static and dynamic response analysis was conducted on analytical models of increasing fidelity in 0g and 1g. Finally, modifications to the existing low-frequency suspension system design were made to allow for testing the very lightweight test model.

INTRODUCTION

This paper describes progress in the concept definition of a lightweight, deployable Synthetic Thinned Aperture Radiometer (STAR) to enable the realization of 10 km resolution global soil moisture and ocean salinity measurements at 1.41 GHz from space.

A high-level operational concept for such a STAR mission was defined in a previous study¹ by researchers at NASA Goddard Space Flight Center. In the study, a comparison was made between STAR antenna diameters and fields-of-view (FOV) required for single and dual spacecraft configurations at various orbital heights. An antenna with 17 m diameter and 37.2 deg FOV was selected in the study based on signal decorrelation limits and an instrument brightness temperature error budget of $\Delta T < 2K$. The antenna would be one part of two spacecraft flying in formation at a 665km orbital altitude as shown in Table 1.

STAR operates passively via interferometric aperture synthesis which was historically used by radio astronomers to map radio sources with high resolution via earth rotation synthesis². In this approach, an array of microwave antenna elements is sparsely distributed over a large aperture. Thus, the thinned aperture radiometer has a collecting area of only 5-10% of an equivalent filled aperture and, as a result, an areal density (kg/m^2) an order of magnitude lower. For the soil moisture application, signals from receivers which operate at the L-Band frequency of 1.41GHz are combined via complex correlation to coherently synthesize an antenna beam from which the science data is retrieved.

The 17 m aperture STAR is the focus of the current scaled model development. As shown in Figure 1, the lightweight concept is a modified tetrahedral geometry with four lightweight, deployable columns emanating from a central hub. Column ends are connected via tension cables to enhance dimensional stability by increasing out of plane stiffness. Microwave sensing elements are supported on a tensioned panel.

The overall objective of the current effort is to mitigate fundamental risks associated with integration of a sparse array of antenna and receiver elements onto a lightweight, tensioned platform that utilizes thin-shell, deployable structural elements. In order to meet this objective, a 1/3-scaled dynamics Phase 0 test article is being developed for concept demonstration and dynamics and control testing. The initial model will be non-deployable but will include lightweight structural elements to create a representative system. The test article will be used to develop methodology and design tools to actively and/or passively control structural shape variations of the ultra-lightweight, large aperture radiometer in order to maintain desired radiometric

performance. In this paper, progress in the development of the Phase 0 test article will be discussed. First, a strategy for selecting and evaluating initial parameters will be presented. Results from several other parallel studies that were conducted to refine the model definition will be presented. In particular, a study was conducted on section (1/3) models of the tensioned panel to optimize geometry of the panel for the most uniform load distribution. Finally, a study to modify an existing low-frequency suspension system for use with lightweight models was performed.

APPROACH

The approach being used in this concept definition study is summarized in Figure 2. Initial design parameters were defined based on analysis of other STAR spacecraft concepts being considered for near-term flight and based on current assessments of radiometric system design specifications for the proposed 10km STAR science mission¹ discussed earlier. Similarity laws were formulated via dimensional analysis of the equations of motion to enable dynamic scaling of the system parameters. Scaling criteria were established and trade studies were performed using the similarity laws to determine the best scaling approach for test model definition. A hybrid scaling approach was used in which subcomponents of the system may be scaled differently than the other system level parameters without introducing significant system level errors. In addition, an initial assessment of the 5-m test model static and dynamic characteristics was performed via hand calculation and non-linear finite element analysis (FEM) for models of increasing fidelity. Based on the results of this analysis and the scaling trade studies, design parameters were revised for further model development.

INITIAL DESIGN PARAMETERS

The goal of scaled model development is to define a physically realizable experimental model that is the physical representation of a full scale spacecraft. Typically, estimates of parameters describing the full scale spacecraft are available and may be used in formulating the design of the scaled test model. For newly innovated concepts, however, such full scale information is rarely available. Thus, parameter estimates must be derived from similar spacecraft and, in the case of far-term concepts like the lightweight STAR concept, from extrapolation of technology advancements to the future.

Design parameters for two near-term STAR missions were identified. The first is the European Soil Moisture and Ocean Salinity (SMOS) Mission³ and the second is a concept being proposed by NASA Goddard Space Flight Center (GSFC)¹. Both concepts use a single spacecraft with deployable panels and sparsely distributed antenna elements for synthetic aperture synthesis. The elements are distributed along three arms which are deployed in a Y-configuration analogous to the lightweight STAR concept being developed in this study. Figures 3 and 4 show concepts of these platforms and Table 2 contains a few relevant system parameters for each mission. Key parameters for design of the test model include spacecraft mass and inertia, first modal frequency, sensing system mass, and radiometric requirements. Key initial design parameters are summarized in Table 3.

Spacecraft Mass and Inertia

As shown in Table 2, the mass of the antenna is about 57.16% of the total spacecraft mass for the GSFC concept and 36.84% for SMOS. Thus, the dynamic behavior of the spacecraft and antenna arms is clearly coupled. Spacecraft maneuvers and environmental disturbances can induce such dynamic response which may interfere with operation of the attitude control system (ACS) if structural response frequencies are in the bandwidth of the controller. These physics can only be studied in the laboratory if the representative mass and inertia properties of the full spacecraft platform are included in the test article. Unfortunately, the spacecraft hub inertial properties for both spacecraft are unknown and an estimate is not yet available for the lightweight STAR concept.

Thus, the focus of the Phase 0 model will be on developing control methods and architectures for modifying the structural shape and motion of the antenna and on simply understanding how to characterize and control the dynamics of a tensioned system. Because the model will be suspended, relative inertial properties of the spacecraft 'hub' to the appendage arms will be considered. However, it will not necessarily be representative of the full scale, lightweight STAR until more definitive inertial information becomes available, perhaps, via additional system study.

First Modal Frequency

The lowest modal response of the each reference spacecraft is assumed to be first bending mode of the long, narrow antenna arms. For the GSFC concept, the design requirement for this first frequency is specified as 0.5 Hz. The first frequency for SMOS is unavailable. Thus, a frequency of 0.5 Hz was used as an initial design target for the full scale STAR. The final frequency requirement to be used for the test model will depend on results of the scaling trade study.

Sensing System Mass Estimate

Technology is being developed to fully integrate antenna sensing system elements and electronics directly into tensioned membranes and/or other lightweight panel structures. For example, a low loss, low mass band-pass filter antenna element with integrated receiving electronics is being developed for passive radiometry to eliminate the need for separate receiving electronics.⁴ Antenna transmission and receiver elements are being developed for integration into tensioned membranes for active synthetic aperture radars (SAR).^{5,6} Further, technology is being realized for miniaturization of power and communication systems and integration of such systems onto thin, lightweight structures.

As near-term missions, the GSFC and SMOS full scale system designs do not include these smaller, lightweight antenna/receiver technologies. For instance, for the GSFC concept, the antenna elements (0.1 kg each) are each supported by receivers (0.25 kg each), and A/D converters (0.1 kg each). Each arm is defined by 6 panels and each panel has 13 antenna elements which are supported by power (1 kg each) and communications boxes (1 kg each). Power and data communication cabling is 1.97 kg per arm. Thus, the total mass of the sensing system is a substantial 49.07 kg per arm. This does not include the mass of the supporting panels or the panel deployment system.

Thus, assumptions will be made for the lightweight STAR development. For an initial estimate, the full scale antenna/receiver element masses will be lumped together at 0.1kg/integrated element until more definitive values can be obtained. Power/communication box mass will be assumed to be 0.1kg as well. In addition, it will be assumed that the 17 m STAR has the same antenna element sizes and spacing as the 27 m STAR since both operate at L-Band (1.4GHz). Thus, fewer elements would be required. The number of antenna/receiver elements per arm required is 49 and the number of panels 4, each with a power/communication element. This will lead to a total sensing element mass for the full scale antenna of 5.3 kg which may still be equal to or exceed the entire lightweight spacecraft mass.

Distributed mass due to power and communication systems will be assumed to be of secondary importance and not critical for meeting the objective of the Phase 0 model. This is due to the technology advances indicated earlier and because no information is available regarding the stiffness and geometry characteristics of such cabling. It is noted, however, that the effect of such systems on the dynamic systems should be considered in the future as the mass of such cabling can equal the mass of the lightweight column which supports it. This distributed mass and stiffness can have a dramatic impact on the system dynamic response.

Radiometric Parameters

Several issues related to dynamic scaling of 'radiometric' requirements must be addressed.

The first is the relative positioning of antenna elements for maximum performance at the 1.400-1.426 GHz band used for soil moisture measurements. According to Table 1, the GSFC Concept requires that the elements are spaced 0.8λ apart for optimal radiometric performance. At 1400 MHz, the λ is 0.21413 meters. Thus, 0.8λ is 0.171314m for the full scale GSFC antenna *and* the 17 m STAR since they both operate at the same wavelength. Thus, for a $\sim 1/3$ scaled test article, the proportional distance is 0.05036 m or 5 cm apart. Further, in order to obtain sufficient bandwidth for soil moisture radiometry, the height of the radiating element above the ground plane for a typical microstrip patch is about 0.254 cm (0.1 inch). The width and length of the element are each approximately 15 cm. Assuming the same dimension for the 17 m STAR, the dimension becomes 4.41 cm for a $\sim 1/3$ (0.294) scaled test model. It is noted that this analysis does not represent a radiometric sub-scaling which would lead to a different result. Here, the scaling is structural and elements are represented by distributed lumped masses on the panel.

The second radiometric parameter is the allowable surface deformation. This will establish a control objective for maintaining desired surface flatness in the presence of spacecraft disturbances. A root mean

square (rms) value of less than $\lambda/20$ is reasonable with a goal of $\lambda/50$. From Table 1, it is seen that for the GSFC concept, the allowable deformation at the end of one arm is $\pm 10\text{mm}$. To obtain the rms value, the antenna arm was assumed to be in the first mode shape deflection. Thus, the first mode deflection for a clamped free beam⁷ scaled by a 10mm end deflection was used to compute an rms value of 5.05 mm or $\lambda/42$. This is within the range indicated. Therefore, the rms value will be selected as $\lambda/50$ or 4.3 mm. Assuming the same requirement for the 17m STAR, a rms surface shape requirement of 1.4 mm will be used for the scaled model. A requirement was not established for relative rotation between elements but may be included pending results of other research in electromagnetics.

It is important to note that in a previous study⁸ it was determined that rms alone is not the most effective indicator of antenna performance. When surface shape modifications are made, the performance metric must include decrements in overall antenna gain (dB) and on radiation side lobe levels (dB). At this time, the resources are not available to evaluate the antenna radiometric performance. Thus, for the Phase 0 model, only rms will be considered as a performance metric.

DYNAMIC SCALING

In order to perform structural characterization of the STAR spacecraft, dynamic scaling was required since the dimensions of the full-size antenna exceeded laboratory space available for testing. Such scaled model development and testing has been performed for many years at NASA Langley Research Center for a variety of different aerospace applications. In all these cases, the significant structural dynamic characteristics are preserved between the full scale and reduced-scale models. This assures that the scaled model is a realistic physical representation of the full scale system. In this study, similarity laws were established and a design trade study was performed ensure that scaling laws lead to physically realizable structural components.

Similarity Laws

Similarity laws were defined by the same approach that was used to define a scaled dynamics and control model for the EOS AM-1 platform at NASA Langley Research Center.^{9,10,11} In this approach, a dimensional analysis was performed on the dynamic equations of motion to establish simple scalar relationships between the full scale model and the scaled model.

A scale factor is simply a scalar number based on similarity laws that describes a particular model characteristic relative to the full scale model. For instance, consider velocity. If the model dimension is scaled by one-half ($\lambda_L=0.5$) and the frequency (1/seconds) is scaled by a factor of 0.5 ($\lambda_{\text{time}}=\lambda_t=2$), then the derived scale factor (ie. similarity law) for velocity is given by

$$\lambda_{\dot{x}} = \frac{\lambda_L}{\lambda_{\text{time}}} = \frac{\dot{x}_{\text{reduced-scale}}}{\dot{x}_{\text{full-scale}}} \quad (1)$$

Thus, the velocity observed on the scaled model will be 0.25 that observed on the full scale model. A "specified" scale factor represents the scaling of a fundamental unit in the physical system. "Derived" similarity parameters are the result of such scaling. A derived scaling law can be obtained for any parameter associated with the physical system if scale factors are specified for all fundamental units in the system.

For the case of dynamic scaling, the similarity laws are derived such that each term in the dynamic equation of motion given by (2) is multiplied by the same scalar coefficient.

$$M\ddot{x} + C\dot{x} + Kx = F \quad (2)$$

Thus,

$$\lambda_M \lambda_{\ddot{x}} = \lambda_C \lambda_{\dot{x}} = \lambda_K \lambda_x = \lambda_F \quad (3)$$

Each of the factors in (3) is either a specified similarity law or a similarity law derived from the specified values to satisfy (3). The same relation holds for the non-dimensional equation of motion as given by

$$\ddot{x} + 2\zeta\omega\dot{x} + \omega^2 x = 0 \quad (4)$$

with

$$\lambda_{\ddot{x}} = \lambda_{\zeta} \lambda_{\omega} \lambda_{\dot{x}} = \lambda_{\omega}^2 \lambda_x \quad (5)$$

For the current study, similarity law equations were generated for a number of system parameters. A spreadsheet design tool was developed and was validated on scale factors generated for the EOS AM-1 model design trade study.⁷ Once similarity laws are established, several different scaling approaches can be used for the system. One type of scaling that is typically used is *replica scaling*. Replica scaled models are geometrically similar to the full scale model and use exactly the same materials at similar locations.⁹ The same materials as in the full scale model are used. Thus, for this type of model, λ_L is specified and λ_M is derived such that $\lambda_\rho = 1$, where ρ is the effective density of the model. Another type of scaling is *multi-parameter scaling*. Multi-parameter scaling is the most general type of scaling in that each unit of the physical system has a specified scale factor.

Scaling Criteria

The art of scaling is in deciding which design parameters are important for adequately capturing the fundamental physics of interest in a reduced scale model. Typically, this is based on insight and experience of the designer. Sufficient parameters must be selected such that significant physical phenomenon is captured in the scaled model. Choosing too few leaves out important dynamics in the scaled model. However, selecting too many parameters could over constrain the problem, making it difficult to design a representative physical system.

To facilitate making decisions about what parameters to use, it is important to keep in mind exactly what the goal of this model development is and make sure that the scaling parameters enable the design of a model to meet that goal. The goal is to design and build a dynamically scaled, non-deployable Phase 0 model of the STAR for controls and dynamics testing. Specifically, the model will be used to develop methodology and design tools to actively and/or passively control structural shape variations of an ultra-lightweight, large aperture antenna to maintain desired radiometric performance. Thus, the set of parameters to be scaled must be sufficient to describe the physics essential to dynamics and controls testing. In addition, the set must include parameters that are useful in actually *building* key hardware components of a physically realizable test article. From this, two criteria were established to select scaling parameters.

1. Parameters must fully describe fundamental physics of interest (*specified*) - Mass, length, time (ie. Frequency) and deflection were identified from dimensional analysis on the dynamic equations of motion to be the parameters which represent the fundamental physics of interest.

2. Parameters must include design parameters of key components to be scaled (*derived*) - The key dynamic components of the test article are the columns and the panel. *Bending Stiffness (EI)* is the key quantity describing elastic behavior of interest for these main structural components. The scale factors for this parameter are based on scale factors selected from the fundamental set of parameters and the scaling for EI is considered a *derived factor*. Selecting a product of design parameters allow scaling without constraining specific design elements of components. For instance, element cross sectional characteristics or modulus may vary in an unscaled manner as long as the scale factor for EI holds. This also allows for alternate lightweight column concepts with the same elastic behavior to be substituted in the model. If the panel is a thin plate, the plate bending stiffness, $D = Eh^3 / 12(1 - \nu^2)$ can be used as a derived factor for scaling. Otherwise, if the plate is a thin membrane, panel tension, elastic modulus and, perhaps, Poisson's ratio can be considered for scaling. Another key system parameter, particularly for rigid body spacecraft control, is Mass Moment of Inertia (I_0).

Scaling Trade Study

Using the similarity law design tool developed, an extensive trade study was conducted to identify the scaling approach most suitable for designing the STAR test model. A number of both replica and multi-parameter scaling approaches were considered for 1/2 and 1/3 scale models of the full scale 17-m STAR. The case selected was based on reasonableness of resulting scale factors and the expected ability to achieve physical realization of the parameters.

Key parameters for the selected case are summarized in Table 4. As indicated earlier, an approximately 1/3 multiple scaling approach was selected in order to achieve a 5-m aperture test article size. In addition, the trade study results showed the benefits of scaling the factor of time since many parameters are affected

by this variation. Ultimately, λ_t was selected as 0.5, which leads to a $\lambda_{freq}=2$. Thus, the test model has modal frequencies twice that which would be observed on the full scale STAR.

Scaling of Lightweight Columns

One of the challenges of dynamically scaling lightweight structural components is that the structures are characteristically very thin at full scale size and are typically an integral part of very large spacecraft concepts. Thus, using a linear geometric scaling approach for formulation of a reduced scale test article leads to unachievable thickness specifications for the lightweight structural components.

An 'EI' Scaling Approach was developed as part of this study which attempts to resolve design difficulties associated with scaling lightweight, thin-walled columns which are subcomponents of a larger, more massive system. The method allows designers the freedom to select cross-sectional geometry most convenient for manufacturing without significant effects on system level dynamic behavior. In order for the EI Scaling Approach to be applicable for scaling a lightweight structural component, the structural mass associated with it must be small relative to the overall system mass. In this case, variations in EI of the lightweight structural component dominate effects due to changes in mass. Hence, small mass changes can be ignored and the EI Scaling Approach is valid. A simple beam example is presented in the Appendix to show this concept. The designer, however, must define an acceptable level of frequency error and monitor variations in mass such that the subcomponent mass does not become a significant mass in the overall spacecraft system. As an example for the current system, Figure 6 shows the system level frequency error due to column mass variation for a system level model of the 5-m STAR to be discussed later. No variation in modal frequency was observed in modes 1-7. Only 5% percent error occurred in frequencies for modes 8-10 due to 25% variation in column mass. Thus, the EI Scaling Approach applies to the current model.

Figures 7 and 8 show results for $\lambda_{EI}=0.0299$ from a design tool that was developed to explore the EI Scaling Approach. All data presented is based on a baseline column thickness for the 5-m STAR test article of $3.05\text{e-}4\text{m}$ and column diameter of 0.127m . Note that in the case discussed, *reverse scaling* is used. Therefore, given initial parameters for the 5-m STAR test model, reasonable parameters for the full scale model are being sought and $1/\lambda_{EI}$ is used.

If E is changed by a factor, Figure 7 shows how diameter and thickness would have to vary in order to maintain the desired scale factor for EI. Thus, when E is increased, the diameter must be smaller for a given thickness since $I=\pi(D/2)^3t$ where "D" is the diameter and "t" is the thickness¹². Similarly, if the thickness is increased, a smaller diameter is needed. So, a range of cross-sectional properties are available for design while maintaining the desired λ_{EI} .

The impact on mass is shown in Figure 8. This diagram presents a ratio of *mass per unit length* between the scaled and unscaled models. Note that this is equivalent to a ratio of areas since the density is not scaled in the EI Scaling Approach. The result of ignoring mass scaling is that the *mass per unit length* ratio varies from a decrease in mass per unit length of 0.87 to an increase of 29.9, depending on the thickness and diameter selected. Figure 8 correlates with Figure 7 and shows that the large mass increases are associated with increasing the thickness even though the diameter becomes smaller.

An extensive trade study was conducted using the EI Scaling Approach to define the most feasible column geometry for the 5-m STAR test model. A $6.4\times10^{-2}\text{m}$ diameter column with $6.1\times10^{-4}\text{m}$ thickness was selected. Using $1/\lambda_{EI} = 1/0.0299$, a full scale diameter of $25.8\times10^{-2}\text{m}$ and a thickness of $3.05\times10^{-4}\text{m}$ were selected as these dimensioned seemed realistically achievable in manufacture for the full scale STAR. The mass ratio calculated was a factor of 2.03 and increased column mass in the system by 11.49% of the overall system mass.

Scaling of Tensioned Panel

A similar hybrid scaling approach may be used for dynamically scaling the tensioned panel depending on whether the panel can be considered a membrane or a shell. In particular, for plates which have deflections many times larger than their thickness, the resistance to plate bending can be neglected. Thus, the flexural rigidity is ignored and the shell problem is reduced to that of a flexible membrane.¹³

For shells, a "D" scaling may be used which is equivalent to the EI Scaling Approach. Since the plate bending stiffness, E, h (thickness) and ν (Poisson's ratio) are available to the designer for scaling as long as λ_D remains constant. A typical design curve is shown in Figure 9 for constant ν . For the membrane case,

the dynamic behavior of tensioned membrane panel in system is stiffness driven via tension and elastic modulus. Small variations in mass due to changes in thickness or density can be neglected since the mass is relatively small within the overall system and the bending stiffness is effectively zero. Figure 10 shows that such mass variation in mass of a thin membrane has no effect on the system level dynamic response of the tensioned panel.

In both scaling cases for the panel, the designer must define an acceptable level of frequency error and monitor variations in mass such that the subcomponent mass does not become a significant mass in the overall spacecraft system. In the case of the current STAR model, the panel design has not yet been finalized. It is apparent that a thin (0.5- 3 μm) tensioned panel will not support the estimated distributed sensing system unless fully integrated, low mass sensing system components are realized. Thus, at this point in the development, the panel is assumed to be a thin panel without instrumentation until a more realistic design refinement can be made.

STRUCTURAL ANALYSIS

Model Description

Two FEM models were used in this study. The first model, Model 1 Version 3 (M1V3), had a hybrid lumped and distributed mass representation of STAR. The model purposefully does not include detail of the tensioned membrane beyond a tensioned cable representation. This allows an initial focus on the platform dynamic behavior without having to focus on resolution of computational issues associated with large area tensioned membrane structures. The second model, Model 2 (M2), had increased fidelity and included a 2000 degree-of-freedom (dof) tensioned panel.

MSC.NASTRAN¹⁴ software was used to perform FEM static and modal analyses with both shell and membrane representations of the panel. A non-linear large displacement solution approach was used to define the system stiffness matrix. The system was pre-tensioned using *mechanical loads* by sub-structuring the system and then applying loads. Sub-structuring is achieved by dividing the structure into tension/compression members. In this case, tension wires and the panel are divided into nine substructures each, for a total of 18 substructures. The columns are one substructure. Multi-Point Constraint (MPC) equations were applied for coincident nodes. For instance, translational and rotational displacements of a structural members are equal but opposite in sign to the ones of an adjacent members. Modal response analysis was performed by ‘restarting’ from the non-linear static analysis.

Initial Static Loads Analysis

Analysis was performed to evaluate static loads acting on the tensioned structure in both 0g and 1g. It is noted that since lightweight columns are designed primarily to support only axial compressive loads, a constraint was required such that the column was not subjected to a bending load at the equilibrium condition. Static loads analyses were performed via vector analysis on an inelastic structure and also using the FEM. Resulting loads are summarized in Table 5.

Vector Analysis

An initial estimate of static loads was hand-computed via vector analysis of a tensioned structure without applied gravity. The structure was assumed to be inelastic and was scaled 1/3 in the linear dimension. The analysis was performed by computing the vector sum of forces at each of the structure’s 6 nodes. Unit vectors were computed for each structural element, including ‘membrane’ cables. These unit vectors were used to compute a vector sum of forces at each node. The unbalanced reaction force was computed as the amount of force away from the axial load direction of the lightweight columns. The long cable tension was iterated upon until the unbalanced load was zero and static equilibrium was achieved at the hub. Tension in the ‘membrane’ cables was assumed at a nominal value of 5N. Zero unbalanced load was achieved in the column when the short column has a 26.02 N compression, the long column had a 17.34 N compression and 13.25 N was in the long tension cables.

FEM Analysis

Analogous static analysis was performed using the elastic FEM model in 0g. The equilibrium solution was obtained by varying beam cable tension until there was no moment in the column due to loading. According to the static FEM analysis, at a panel tension of 5N, the short column has a 26.5 N compression, the long column has a 17.37 N compression load and there is 13.3 N in the long tension cables. These results are identical to those obtained for the inelastic structure via vector analysis. This not only verifies results but also indicates that little distortion of the elastic structure occurs due to such static loading. In 1g, the system static loads increase to accommodate the uniform gravity loading as summarized in Table 5.

Panel Geometry Trade Study

An analytical tensioned panel trade study via FEM analysis was performed to identify a panel geometry with optimal tension distribution. The model used was a 1/3 'symmetric' subsection of the tensioned panel without support structures since using only a subsection of the panel significantly reduced computation time and model complexity. In each case, only in-plane translation was constrained for symmetric boundary condition. Both shell and membrane models were evaluated where convergence could be achieved. Three geometries B, C, and E were considered and a single panel geometry was down-selected for further development.

For Geometry B, it was observed that tension input at the panel attachment point was not evenly distributed and caused highly concentrated displacement along a line to the panel center. The geometry also caused increased panel center buckling in 0g and unsupported edges in 1G, even with tension wires along panel edges. In general, small diameter tension wires along panel edges did not improve results but increased time for numerical convergence of the FEM solution. Results for Geometry B with 5N tension in the panel in 1g and 0g are shown in Figures 11, 12, and 13.

For Geometry C, the edge tension wires caused uneven tension distribution in 0g and increased panel center buckling in both 1g (Tension Wire Diameter = 2.5e-6m) and 0g (Tension Wire Diameter = 5e-5m). Without the edge tension wires, no center displacement occurred for the 0g case and an even load distribution was observed for the 1g case. Results for Geometry C are shown in Figures 14, 15, and 16.

Geometry E results are shown in Figures 17 and 18. The results show that displacement in 1g is dominated by normal translation. In 0g, displacement is dominated by panel extension under tension load. In fact, the extension is so large that the 5N goal for tension in the panel could not be met due to strain of the panel exceeded geometric constraints. Only cases with the shell representation of the panel converged. High tension cases demonstrated lateral buckling for the thin panel material as shown in Figure 18. In fact, all static analyses for this geometry indicated that the panel is highly susceptible to wrinkling. Finally, all cases with cables along the panel edges diverged.

In summary, Geometry C was down-selected for further development due to uniform load distribution observed in the panel analysis.

Static and Dynamic Analysis

The static responses of model M2 with a Geometry C panel are shown in Figures 19 and 20 for 0g and 1g, respectively. The zero center panel displacement in the 0g case indicates an even distribution of the 5N tension in the panel. In 1g, static center panel displacement is 0.0471m while the panel is under 5N tension. The displacement is 1% the antenna diameter.

Modal response of the model in 0g is summarized in Figure 21 and Table 6. The first mode is first panel bending. The second mode is in-plane torsion that involves the long columns of the model. Higher modes are repeated, each 3 times. For a comparative 1g analysis, the model was initially constrained via a light spring at the base of the model. Modal response is shown in Figure 22. The first dynamic mode is an in-plane torsion. The second mode involves side flapping of the tensioned panel. Stiffening due to the addition of gravity has shifted the first panel bending mode to mode 4.

SUSPENSION SYSTEM DESIGN TRADE STUDY

A suspension system trade study was performed to evaluate the suitability of a currently available low frequency model suspension system used for dynamics and control testing. The current system is configured for test models which weigh two orders of magnitude higher (~500 kg) than the lightweight

STAR (<15 kg). For performance the evaluation, the suspension system was integrated with the Model 2 and analyzed via FEM.

Without modification to the system design, the first suspension system frequency occurred at 0.11 Hz as expected and the first panel mode occurred at 3.58 Hz. Nearly 60 'guitar string' modes occurred between these two frequencies. To eliminate the guitar string modes, an analytical configuration trade study was conducted. In this study, multiple independent suspension points, multiple suspension points with cross connections, a single suspension with multiple attachment points, added mass (2x model mass), and hybrid cables (steel and kevlar combinations) were evaluated.

Results showed that a single point suspension with multiple attachment points minimized repeated frequencies due to suspension system dynamics. Added mass (2x model mass) significantly reduced number of low frequency modes of upper suspension system. The use of higher stiffness steel for lower suspension cables reduced combined model and suspension system dynamics. Distributed mass via an in-line massive 'bell' decreased modal activity in lower suspension cables.

A hybrid cable system was selected with a 15 kg added mass suspended at 5 m above the test article as shown in Figure 23. The resulting configuration showed the fewest suspension system dynamics below the first flexible body frequency of interest and reduced interaction with the other low frequency flexible body modes. Modal frequencies for the suspended system are shown in Table 6. The first panel mode is at mode 20.

Static loads on the suspended model are given in Tables 5. Panel center displacement of the suspended model under 1g is 11.4 cm. Loads in both the long tension cable and short column increase by a factor of approximately 6 compared to the 0g case. Long column compression increases by a factor of about 5. In 0g, the long column bending moment is 0 n-m. The long column bending moment increases to -1.22 n-m for the '0g to 1g' configuration which is supported only at the base of the model. For the three point suspension in 1g, the maximum long column bending moment is 6.91e-1 n-m.

CONCLUSIONS

In this study, initial design parameters were established and a hybrid scaling approach using multi-parameter scaling was selected for designing the reduced-scale test model parameters. A tensioned panel geometry was selected based on analysis on a 1/3 section of the tensioned panel for optimal load distribution. Static and dynamic analysis was performed on the scaled test model to characterize the structural behavior of the system in 0g and 1g environments. A modification required to enable a current low-frequency suspension system to be used for testing extremely lightweight test articles (<15 kg) was analyzed. In summary, initial analytical studies show that the scaled model development of a 17m STAR is feasible.

REFERENCES

1. Pellerano, F.A., O'Neill, P.O., Dod, L., "Architecture Trade Study for Passive 10km Soil Moisture Measurements from Low-Earth Orbit," IEEE International Geoscience and Remote Sensing Symposium, Sidney, Australia, 2001.
2. Swenson, G.W. and Mathur, N.C., "The Interferometer in Radio Astronomy," Proceedings of IEEE, Vol. 56, No. 12, 1968, pp. 2114-2130.
3. Kerr, Y.H., Font, J., Waldteufel, P., and Berger, M., "The Soil Moisture and Ocean Salinity Mission - SMOS," *Earth Observation Quarterly*, Vol. 66, pp. 18-26, 2000.
4. Piepmeier, J.R., Pellerano, F.A., et al, "Synthetic Thinned Aperture Radiometry (STAR) Technologies Enabling 10-km Soil Moisture Remote Sensing From Space," NASA Earth Science Technology Conference, Pasadena, CA, June 11-13, 2002.
5. Moussessian, A., et al, "Transmit/Receiver Membranes for Large Aperture Scanning Phase Arrays," NASA ESTO Workshop, 2002.
6. Huang, J., et al, "Development of Inflatable Array Antennas," IEEE Aerospace Conference, Big Sky, Montana, March, 2000.
7. Blevins, R.D., "Formulas for Natural Frequency and Mode Shape," p. 158, Krieger Pub. Co, Malabar, FL, 2001.
8. Padula, S.L., Adelman, H. M., Bailey, M.C., "Integrated Structure Electromagnetic Optimization of Large Space Antenna Reflectors," NASA TM 89110, Feb. 1987.

9. Baker, W.E., Westine, P.S., Dodge, F.T., Similarity Methods in Engineering Dynamics: Theory and Practice of Scale Modeling, Hayden Book Co., Inc., Rochelle, NJ, 1973.
10. Sedov, L.I., Similarity and Dimensional Methods in Mechanics, New York, Academic Press, 1959.
11. Gronet, M.J., Davis, D.A., and Tan, M.K., "Development of the CSI Phase-3 Evolutionary Model Testbed," NASA Contractor Report 4630, October, 1994.
12. Lake, M.S. and Mikulas, M. M., "Buckling and Vibration Analysis of a Simply Supported Column with a Piecewise Constant Cross Section," NASA Technical Paper 3090, March, 1991, p.4.
13. Timoshenko, S. and Woiowsky-Krieger, S., Theory of Plates and Shells, 2nd addition, McGraw-Hill Book Co, 1959.
14. MSC Software Corporation, Los Angeles, CA.
15. Craig, R. R., Jr., "Structural Dynamics: An Introduction to Computer Methods," John Wiley and Sons, Inc., New York, 1981, p215.

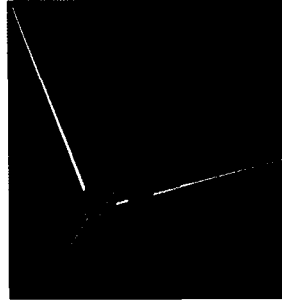


Figure 1. Pro-Engineer Model of STAR in Fully Deployed State

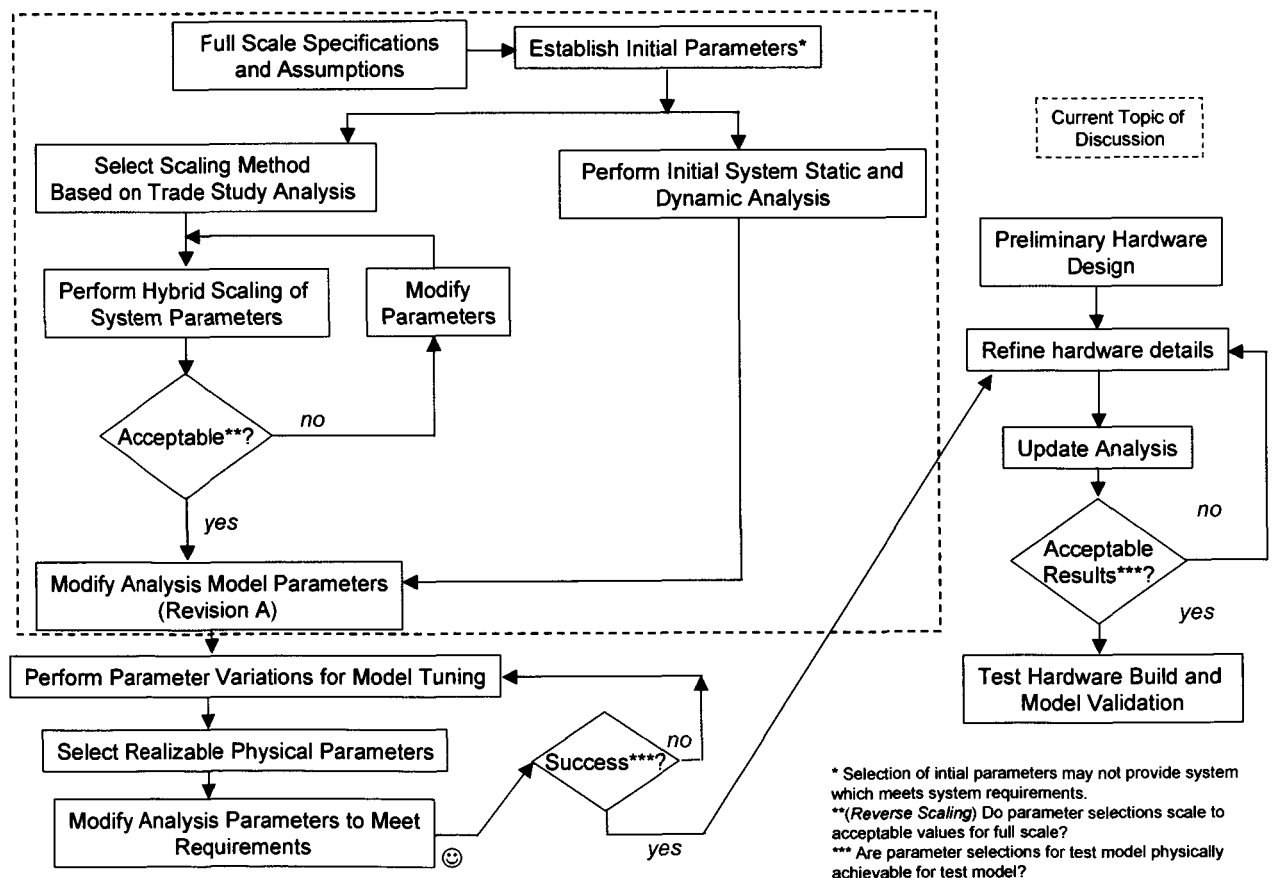


Figure 2 Methodology of Phase 0 Scaled Model Development

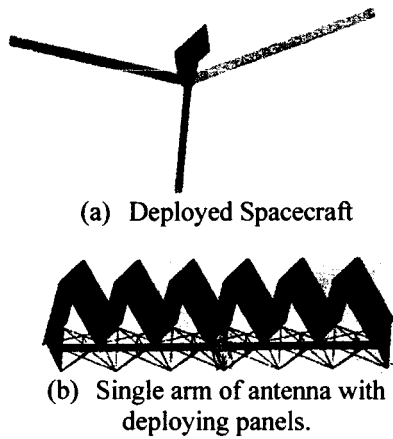


Figure 3 NASA GSFC STAR Concept with Deployable Panels



Figure 4 European Soil Moisture and Ocean Salinity (SMOS) Mission on Proteus Platform

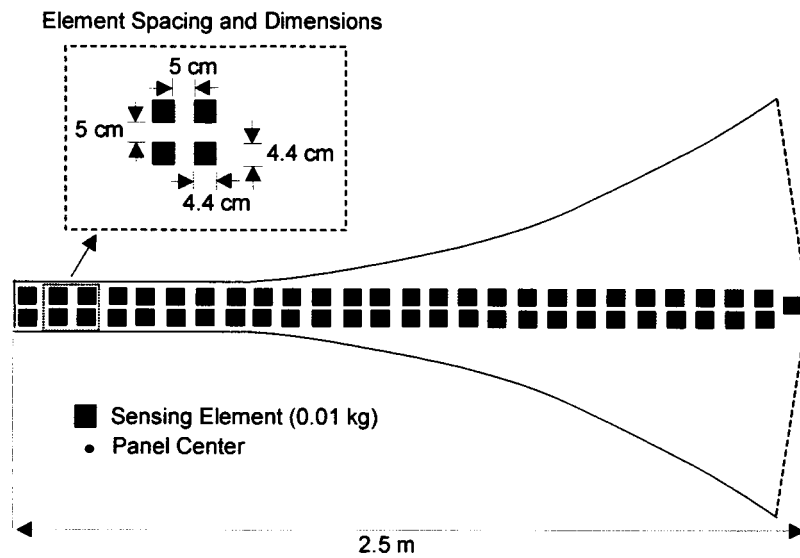


Figure 5 Radiometric Element Distribution on Single Panel Arm

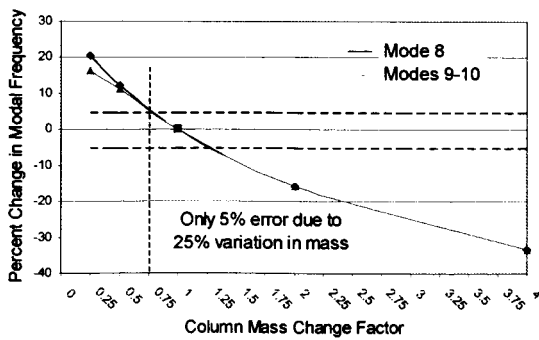


Figure 6. System Level Frequency Variation with Column Mass Change

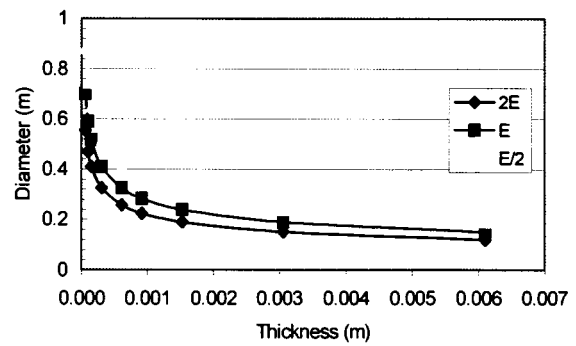


Figure 7 Diameter for $\lambda_{EI}=0.0299$ as Elastic Modulus and Thickness Vary

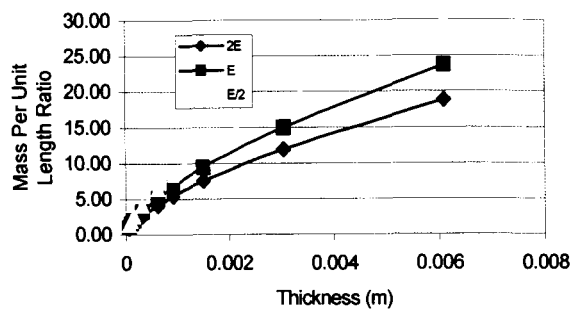


Figure 8 Mass Per Unit Length Variation for $\lambda_{EI}=0.0299$ with Elastic Modulus and Thickness

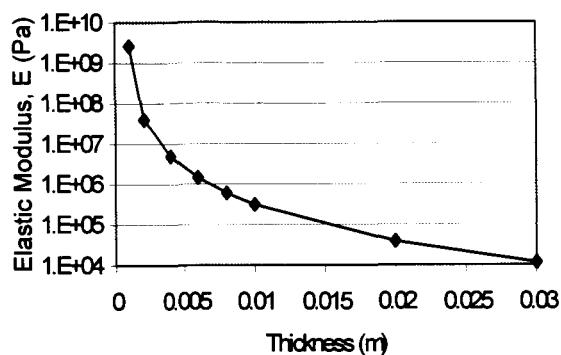


Figure 9 "D" Scaling for Shell Panel ($\lambda_D=0.1195$)

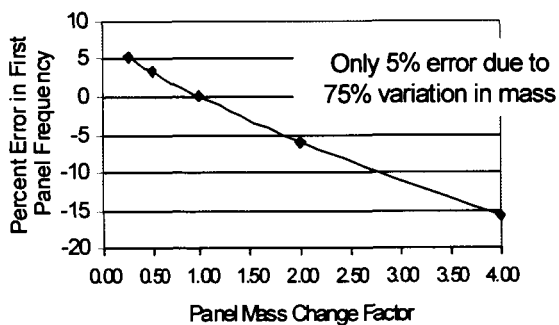


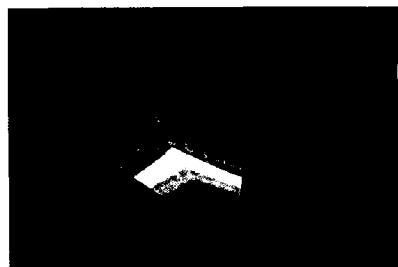
Figure 10 Variation of First Panel Mode Frequency in 0g with Changes in Mass of Membrane (M1V3)



Figure 11 Panel Geometry B : Panel Subsection

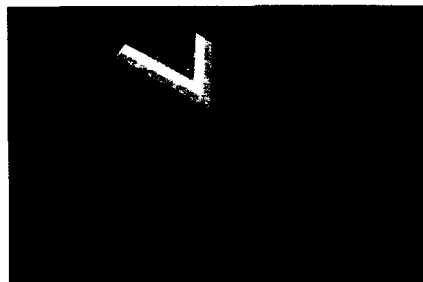


a) 0g

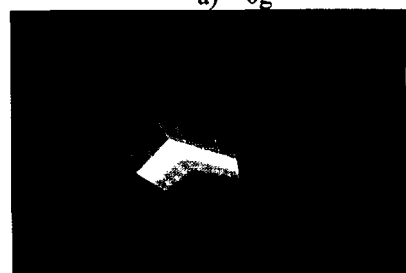


b) 1g

Figure 12 Total Displacement of Panel Geometry B under 5N Tension w/ Edge Cables



a) 0g



b) 1g

Figure 13 Total Displacement of Panel Geometry B under 5N Tension without Edge Cables

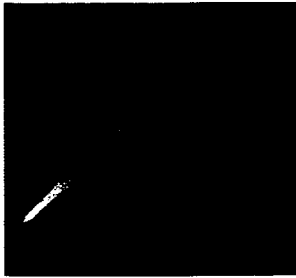


Figure 14 Panel Geometry C: Panel Subsection

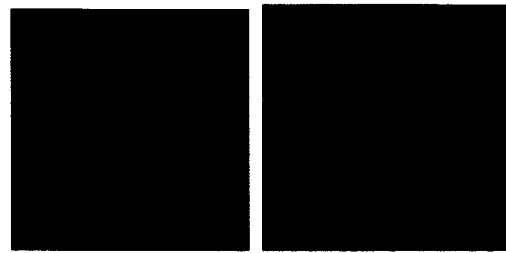


Figure 17 Panel Geometry E: Panel Subsection

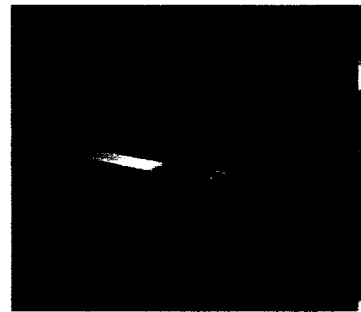


a) 0-g

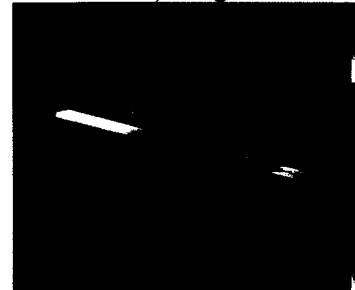


b) 1g

Figure 15 Total Displacement of Panel Geometry C under 5N with Edge Cables

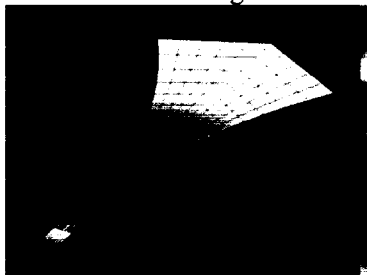


a) 0-g

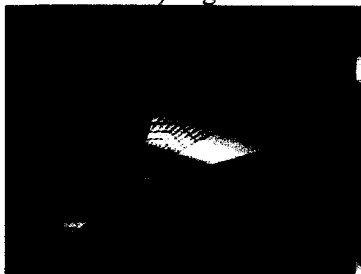


b) 1-g

Figure 18 Total Displacement of Panel Geometry E without Edge Cables



a) 0- g

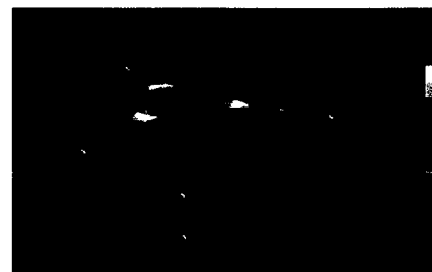


b) 1-g

Figure 16 Total Displacement of Panel Geometry C under 5N without Edge Cables



Figure 19 Static Displacement of the 5-m model in 0g showing no panel center displacement



a) First Mode: 1.6 Hz



b) Second Mode: 1.63 Hz

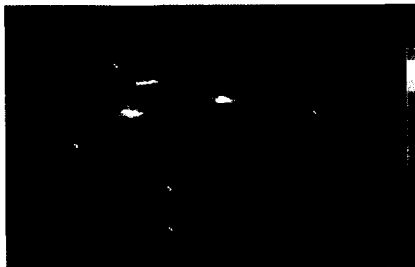
Figure 20 First 2 modes of the 5-m model in 0g



Figure 21 Static Displacement of the 5-m model in 0g to 1g showing 0.0471 m panel center displacement



a) First Mode: 1.63 Hz

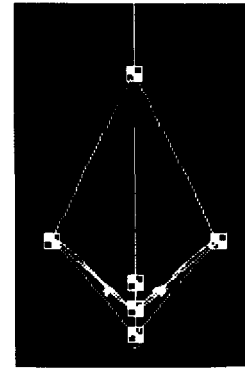
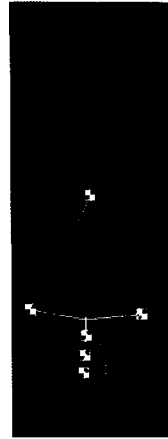


b) Second Mode: 2.62 Hz



c) Fourth Mode: 2.7 Hz

Figure 22 First 3 modes of 5-m model in 0g to 1g



a) 1st Mode: 0.132 Hz Kevlar Cables Top and Bottom
15 kg Mass Bell (0.001m thick)

b) 1st Panel Mode 8 3.695 Hz*

Figure 23 Modal Results for Single Suspension with Multiple Attachment Points

Table 1 STAR Science Mission Concept

Complete Global Mapping within the revisit time interval without data gaps
3 Day Revisit Time
Dual Spacecraft
666 km Orbit Altitude
17.2 m diameter aperture
$\Delta T = 0.76$ K (assumes pixel averaging)
Spatial Resolution: 10km (edge) and 8.21km (nadir)
Soil Moisture Retrieval Accuracy of 4% volumetric or better $\geq 65\%$ of land surface
Mission life of 2 years or longer
1.41 GHz

Table 4 Selected and Derived Scale Factor for Full to Reduced Scale Models

Parameter	1/3 Multi-Scaled
Selected Factors	
Mass (Weight), λ_m	0.294
Length, λ_l	0.294
Time (1/freq), λ_t	0.5
Deflection, λ_x	0.294
Derived Factors	
Bending Rigidity, EI	0.0299
Plate Bending Stiffness, D	0.1195

Table 2 STAR Soil Moisture Measurement
Spacecraft Design Parameters

	GSFC Concept	European SMOS
Launch Date	2008	2006
Horizontal Measurement Resolution (km)	10	50
Aperture Diameter (m)	27	6.75
Antenna Mass (kg)	301	175
Spacecraft Total Mass (kg)	526.6	475
Number Sensing Elements Per Arm	78	24
Linear Spacing of Sensing Elements (m)	0.8λ	n/a
First Frequency (Hz)	0.5	n/a
Max Tip Deflection (m)	+10mm	n/a
Areal Density (kg/m ²)	0.53	4.89

Table 3 Key Initial Design Specifications

Dimension	Reduced Scale	Full Scale
Aperture Size (m)	5	17
Long Column (m)	2.89	9.81
Short Column (m)	0.72	2.45
Avg. Column Diameter (m)	0.064	0.258
Wall Thickness (m)	6.10E-04	3.05E-04
Mass		
Hub (kg)	1.00	3.40
Panel Nodes (kg) (Total)	2.00	6.80
Panel (kg)	0.30	1.02
Long Column (kg)	0.29	1.99
Short Column (kg)	0.07	0.50
Mass w/o Sensing System	4.6	18.92
Mass w/ Sensing System	6.15	24.22
Areal Density (kg/m²)	0.31	0.11
λ/50 RMS (mm)	1.4	4.3

Appendix: Cantilever Beam Example

The transverse vibration of a slender beam with distributed mass and a concentrated tip mass is analyzed. A diagram of this system is shown in Figure A-1. The approximate first frequency of vibration of this system is given by

$$f_1 (\text{Hz}) = \frac{1}{2\pi} \left(\frac{3EI}{L^3(M + 0.24M_b)} \right)^{1/2} \quad (\text{A-1})$$

In [4] this relation was indicated to be within about 1% of the exact solution. Parameters for this problem are given in Table A-1. The beam is assumed to be a thin-walled cylinder. Thus, the cross-sectional inertia, I , is approximated by $I = \pi R^3 t$ and the cross-sectional area by $A = 2\pi R t$.

Table 5 Static Loads on 5-m STAR
Maximum Tension Load (N)

Element	0g	0g to 1g*	1g suspended
Panel	5.0	12.3	5.0
Long Column	-17.4	-23.3	-86.0
Short Column	-26.5	-59.2	-152.0
Long Cable	13.3	9.4	81.0
Panel Center Displ (cm)	0.0	-4.7	-11.4

* low stiffness attachment at base

Table 6 Modal Frequencies of 5-m STAR

Frequency (Hz)	0g	0g to 1g*	1g suspended
Mode 1	1.59**	1.63	0.127
Mode 2	1.63	2.63	0.127
Mode 3	2.88	2.63	0.238
Mode 4	2.88	2.7**	0.26
Mode 5	3.15	3.38	0.26
Mode 6	3.15	3.38	1.42
Mode 7	3.22	3.98	1.42
Mode 8	4.11	4.03	1.42
Mode 9	4.11	4.03	1.45
Mode 10	4.4	5.15	1.45
Mode 20			3.71**

* low stiffness attachment at base

** first panel mode

In this example, the tip mass was varied for a range of column masses that could be obtained for the given single cross-sectional geometry via material density variations (mass per unit length of 0 to 0.2 kg/m). Tip masses used were 1, 10 and 50 kg. The first frequency for each configuration was calculated via (A-1). For each tip mass case, the frequency computed using 0 kg column mass was considered as baseline and ratios of frequencies compared to this baseline were computed as column mass increased.

Figure A-2 shows that the frequency ratio is decreased by about 1% as the mass ratio of column to tip masses approaches about 8.5%. Since the three cases presented are based on three different values of tip mass, the result is independent of the absolute column and tip masses but rather dependent on their ratio. Thus, for this example, 8.5% is a good upper limit estimate for when the EI Scaling Approach could be used to scale the lightweight structural element. While this example is simple, the upper limit may be generalized to more complex structures with small mass ratios between lightweight structural components and the rest of the system. A more conservative estimate might be 6-8%.

However, the designer should understand and

perhaps bound frequency error due to mass changes for each unique system. The acceptable level of frequency error may be a function of factors such as how closely space modes are, whether modal switching occurs with parameter variation, or if scaled model resolution is specified.

In summary, this analysis shows that if the criteria for λ_{EI} can be met via a variation in the cross-sectional thickness and column diameter, the mass variation due to such changes can be regarded as insignificant when the ratio of the lightweight component mass to the system mass remains low. Furthermore, the thickness and column diameter do not need to be linearly scaled by the same factor as the rest of the structure as long as λ_{EI} is met. This provides the freedom required for the designer to choose thickness, diameter, elastic modulus and column material density that can be most reasonably used for the development of dynamically scaled test-articles. Further, this approach is more viable than the constant thickness approach as it preserves a key dynamic characteristic of the structural element rather than discarding both stiffness and mass considerations.

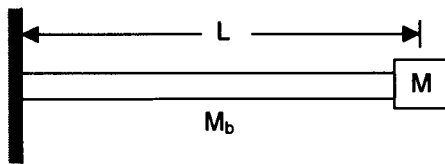


Figure A-1 Slender Beam with Distributed Mass and Concentrated Tip Mass

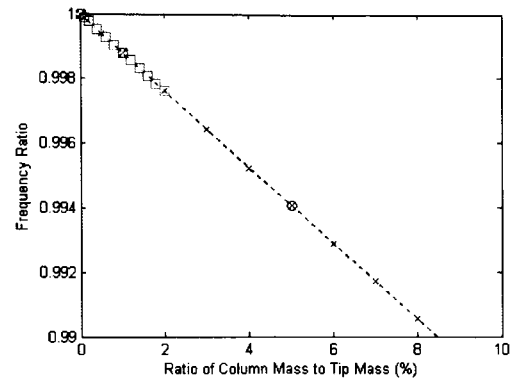


Figure A-2 Frequency Ratio as a Function of Mass Ratio

Table A-1 Parameters for Beam Example

Parameter	Value
L (m)	5
ρ (kg/m ³)	822.3
Thickness of Column (m)	3.05E-04
Diameter of Column (m)	0.127
Modulus of Elasticity, E (Pa)	1.38E+10

REPORT DOCUMENTATION PAGE					Form Approved OMB No. 0704-0188	
<p>The public reporting burden for this collection of information is estimated to average 1 hour per response, including the time for reviewing instructions, searching existing data sources, gathering and maintaining the data needed, and completing and reviewing the collection of information. Send comments regarding this burden estimate or any other aspect of this collection of information, including suggestions for reducing this burden, to Department of Defense, Washington Headquarters Services, Directorate for Information Operations and Reports (0704-0188), 1215 Jefferson Davis Highway, Suite 1204, Arlington, VA 22202-4302. Respondents should be aware that notwithstanding any other provision of law, no person shall be subject to any penalty for failing to comply with a collection of information if it does not display a currently valid OMB control number.</p> <p>PLEASE DO NOT RETURN YOUR FORM TO THE ABOVE ADDRESS.</p>						
1. REPORT DATE (DD-MM-YYYY) 01- 09 - 2003		2. REPORT TYPE Technical Memorandum		3. DATES COVERED (From - To)		
4. TITLE AND SUBTITLE Progress in the Phase 0 Model Development of a STAR Concept for Dynamics and Control Testing				5a. CONTRACT NUMBER		
				5b. GRANT NUMBER		
				5c. PROGRAM ELEMENT NUMBER		
6. AUTHOR(S) Woods-Vedeler, Jessica A.; and Armand, Sasan C.				5d. PROJECT NUMBER		
				5e. TASK NUMBER		
				5f. WORK UNIT NUMBER 23-755-06-00		
7. PERFORMING ORGANIZATION NAME(S) AND ADDRESS(ES) NASA Langley Research Center Hampton, VA 23681-2199				8. PERFORMING ORGANIZATION REPORT NUMBER L-19002		
9. SPONSORING/MONITORING AGENCY NAME(S) AND ADDRESS(ES) National Aeronautics and Space Administration Washington, DC 20546-0001				10. SPONSOR/MONITOR'S ACRONYM(S) NASA		
				11. SPONSOR/MONITOR'S REPORT NUMBER(S) NASA/TM-2003-212645		
12. DISTRIBUTION/AVAILABILITY STATEMENT Unclassified - Unlimited Subject Category 39 Availability: NASA CASI (301) 621-0390 Distribution: Standard						
13. SUPPLEMENTARY NOTES An electronic version can be found at http://techreports.larc.nasa.gov/ltrs/ or http://ntrs.nasa.gov						
14. ABSTRACT The paper describes progress in the development of a lightweight, deployable passive Synthetic Thinned Aperture Radiometer (STAR). The spacecraft concept presented will enable the realization of 10 km resolution global soil moisture and ocean salinity measurements at 1.41 GHz. The focus of this work was on definition of an approximately 1/3-scaled, 5-meter Phase 0 test article for concept demonstration and dynamics and control testing. Design requirements, parameters and a multi-parameter, hybrid scaling approach for the dynamically scaled test model were established. The EI Scaling Approach that was established allows designers freedom to define the cross section of scaled, lightweight structural components that is most convenient for manufacturing when the mass of the component is small compared to the overall system mass. Static and dynamic response analysis was conducted on analytical models to evaluate system level performance and to optimize panel geometry for optimal tension load distribution.						
15. SUBJECT TERMS STAR; Synthetic Thinned Aperture Radiometer; Deployable; Lightweight; Ocean salinity; Radiometry; Soil moisture; Space structures; Tensioned; Tetrahedron						
16. SECURITY CLASSIFICATION OF:			17. LIMITATION OF ABSTRACT	18. NUMBER OF PAGES	19a. NAME OF RESPONSIBLE PERSON	
a. REPORT	b. ABSTRACT	c. THIS PAGE			STI Help Desk (email: help@sti.nasa.gov)	
U	U	U	UU	21	19b. TELEPHONE NUMBER (Include area code) (301) 621-0390	